Intramolecular Proton Transfer in Glycine Radical Cation

L. Rodríguez-Santiago, M. Sodupe, A. Oliva, and J. Bertran*

Departament de Química, Facultat de Ciencies, Universitat Autònoma de Barcelona, Bellaterra 08193 Spain

Received: July 15, 1999; In Final Form: December 4, 1999

The effect of ionization on the relative stabilities of the four lowest conformers of glycine and on the intramolecular proton transfer process has been studied using density functional and MP2 methods. Single-point calculations at the CCSD(T) level have also been performed. The energy ordering of the radical cations differs from that observed for the neutral conformers, mainly due to the changes in the basic and acid character of the NH_2 group upon ionization. Ionization favors the intramolecular proton-transfer process. For the ground ionic state, $^2A'$, both reactant and product have similar energies, the energy barrier being about 9.0 kcal/mol. For the first excited state, the proton transfer appears to be spontaneous. However, in both cases, the final product is a distonic [$NH_3^+-CH_2-COO^\bullet$] radical cation. This is in contrast to what is observed for neutral glycine, for which the zwitterionic structure is not stable in the gas phase.

Introduction

Hydrogen bonded systems are of great importance in biology. In particular, the presence of hydrogen bonds in amino acids, and the polarity of them, are important for the final three-dimensional structure in proteins. On the other hand, intramolecular hydrogen transfer is one of the simplest and most important reactions in biological chemistry, and is a key process in many biological systems. Glycine is the simplest amino acid and is a suitable model to perform studies of biological interest. In particular, the intramolecular hydrogen transfer is an important process given that it relates the zwitterionic and neutral structures of the amino acid. It is well-known that in solution the predominant form of glycine is the zwitterion and in the gas phase only the neutral form exists. Hydrogen transfer in glycine has been extensively studied theoretically in solution.[1−5] In the gas phase, the potential energy surface of the neutral form has been profusely studied theoretically,[6−18] but only few theoretical studies consider the zwitterionic form.[19−20]

The effects of oxidative damage in proteins has attracted much interest in the past few years.[21] Oxidation can be initiated by oxidizing agents such as $OH^\bullet$ or other radicals,[22−25] metal reactions, or ionized radiation[26] and may cause drastic effects in proteins. This process is related to the loss of activity of enzymes which is involved in numerous pathological disorders[22] and in the process of aging. The oxidizing agent induces the oxidation of an amino acid of the peptidic chain; however, the number of studies of radical cations of amino acids is surprisingly small.

Since oxidation can cause important effects in proteins and it takes place in amino acids, it is interesting to study the effect of ionization upon the hydrogen transfer process in glycine. This is viewed as a first step to understanding the proton-transfer process in more realistic peptidic systems. Although several studies exists for glycine derived radicals,[27−33] to our knowledge, nobody has considered the proton-transfer process in glycine radical cation.

In the present work, we study the ionization process of the lowest four conformers of glycine. In particular, we will focus our attention on the intramolecular proton-transfer process of the second conformer in the ground and first excited states of glycine radical cation. We will show that, whereas in the excited state the proton transfer occurs spontaneously, in the $^2A'$ ground state the process is more complex and an energy barrier appears.

Methods

Molecular geometries and harmonic vibrational frequencies of the considered structures have been obtained using density functional methods. The adequacy of density functional methods for the study of the conformational behavior of glycine and other amino acids has been the subject of several recent papers.[13,16,18] It has been shown that the hybrid methods, in particular the B3LYP one, provide very similar structural parameters as compared with MP2 and that the density functional vibrational frequencies and intensities are in excellent agreement with the experimental data.

Moreover, for different radical cations, the UB3LYP method has been shown to perform much better than the more computationally demanding UMP2 one,[34] due to the fact that the perturbation expansion converges slowly when the UHF reference function has large spin contamination. In contrast, UB3LYP does not overestimate spin polarization, which has been related to spin contamination.[35] However, in certain special cases, such as symmetrical radical cations, the DFT method has been shown to overestimate the stability of these hemibonded systems.[36−39] This is attributed to an overestimation by the exchange functional of the self-interaction part of the exchange energy due to the delocalized electron hole.[36] This error is partially corrected by mixing the exact exchange in the functional, the BHLYP method being the one that provides better agreement with post Hartree−Fock methods.[36] Because of that, in this study the calculations have been done using both the BHLYP and B3LYP levels of theory. In both cases, the correlation functional is that of Lee, Yang, and Parr (LYP).[40] For exchange, we use two different nonlocal functionals, the Becke's three parameter (B3)[41] and the Becke's half and half (BH)[42] functionals.

Furthermore, to confirm the density functional results, we have optimized some of the systems at the MP2 level and performed single-point calculations at the coupled cluster level with single and double excitations and a perturbative estimate

10.1021/jp992414o CCC: $19.00
Published on Web 01/25/2000

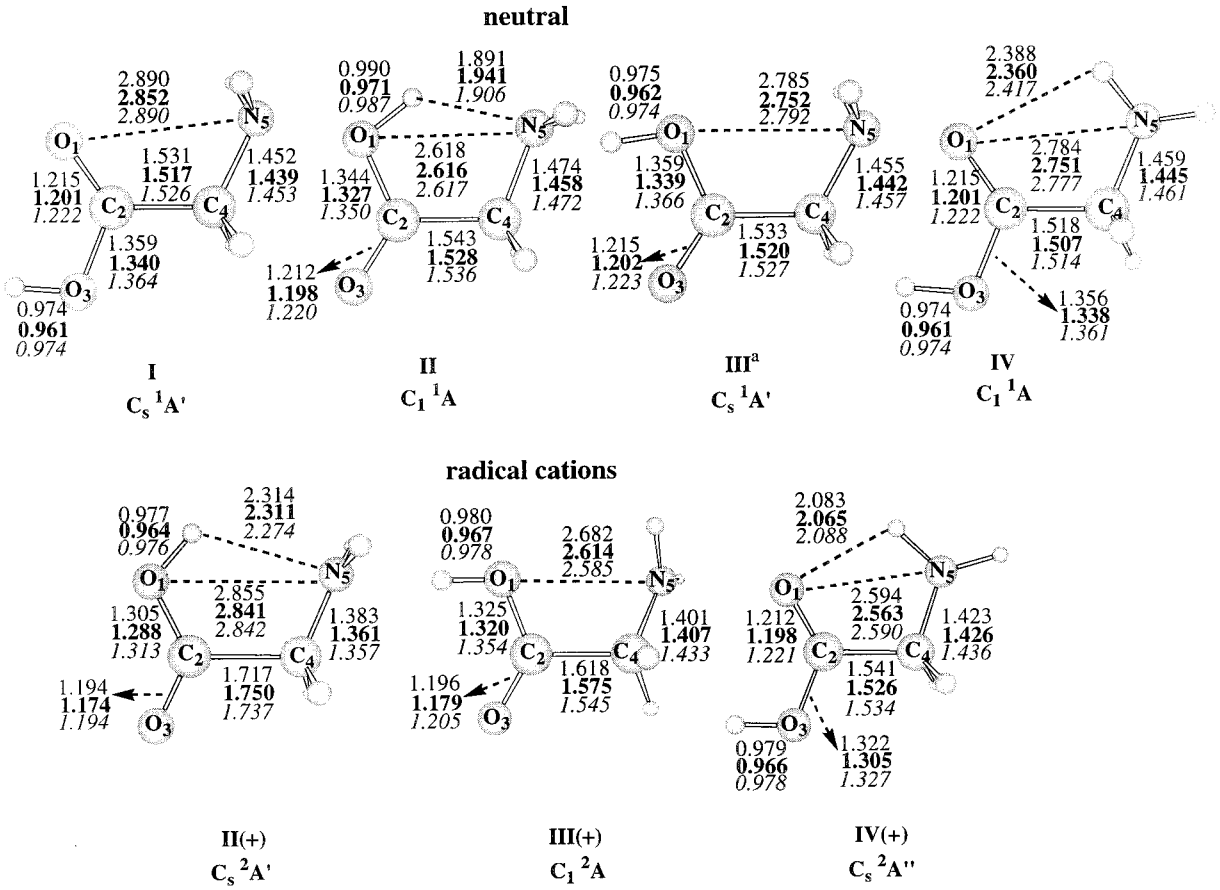

Figure 1. B3LYP, **BHLYP**, and *MP2* optimized geometries of the different stationary points found for glycine and glycine radical cation. Distances are in angstroms and angles are in degrees. [a]C_1 symmetry at the MP2 level.

of the triple excitations (CCSD(T)).[43] It is worth noting that the spin contamination in the studied systems is small, the value of S^2 being always smaller than 0.80. In these calculations, we have correlated all the electrons except the 1s-like ones.

Geometry optimizations and frequency calculations have been performed using the following basis sets. For C, N, and O, we used the (9s 5p)/[4s 2p] set developed by Dunning[44] from the primitive set of Huzinaga supplemented with a set of diffuse sp functions ($\alpha = 0.0438$ for carbon, $\alpha = 0.0639$ for nitrogen, and $\alpha = 0.0845$ for oxygen) and one 3d polarization function ($\alpha = 0.75$ for carbon, $\alpha = 0.80$ for nitrogen, and $\alpha = 0.85$ for oxygen). For H, the basis set used is the (4s)/[2s] set of Dunning[44] supplemented with a diffuse function ($\alpha = 0.036$) and a p polarization function ($\alpha = 1.00$). This basis set is referred to as D95++(d,p) in the Gaussian 94[45] program system. Given that some discrepancies between the B3LYP and CCSD-(T) levels appear when using this basis set, we have also performed calculations using the 6-311+G(3df,2p) basis, which is largely accepted to provide very good results with the B3LYP method.

Net atomic charges and spin densities have been obtained using the natural population analysis of Weinhold et al.[46] Density functional calculations have been performed with the Gaussian 94 package.[45] Open-shell calculations at the CCSD(T) level have been carried out with the MOLPRO-98 program since it allows using a spin restricted formalism RCCSD(T).[47]

Results and Discussion

I. Equilibrium Geometries, Relative Energies, and Ionization Potentials. Figure 1 presents the optimized geometry parameters of the four lowest conformers of neutral glycine at different levels of calculation. Structures **I** and **III** show a bifurcated hydrogen bond between the NH_2 group and the carbonylic or hydroxylic oxygen, respectively. The lowest one (**I**) has C_s symmetry at all levels of calculation. However, structure **III** is determined to be C_s at the B3LYP and BHLYP levels and C_1 at the MP2 one. Nevertheless, the energy difference between the C_s and C_1 structures of **III** at the MP2 level is very small, less than 0.1 kcal/mol. The second structure (**II**) has C_1 symmetry with the hydroxylic group acting as a proton donor and the amino group acting as a proton acceptor. Finally, structure **IV** has C_1 symmetry with the NH_2 acting as a proton donor and the carbonylic group as a proton acceptor.

The absolute and relative energies of these four structures are given in Table 1. As found previously,[11,12,18,48,49] structure **I** is the global minimum of the potential energy surface and structure **II** is found to be the second most stable conformer. Although the obtained geometry parameters are very similar with all methods and in good agreement with those reported at the CCSD level,[12] the computed energy difference between **I** and **II** is underestimated at the B3LYP (0.24 kcal/mol) and MP2 (0.53 kcal/mol) levels of theory, compared to the experimental value (1.0 ± 0.5 kcal/mol).[16,50] However, single-point calculations at the CCSD(T) level, using the B3LYP or MP2 geometries, provide values of 0.97 and 0.88 kcal/mol, respectively, which are in much better agreement with the experimental energy difference and with the CCSD(T) value using CCSD geometries (1.09 kcal/mol).[12] It is interesting to note that the BHLYP density functional provides a value of 1.01 kcal/mol, performing better than the B3LYP approach.

Structures **III** and **IV** are very close in energy and lie about 1.5 kcal/mol above the ground structure **I**. With all methods,

TABLE 1: Absolute (in au) and Relative Energies (in kcal/mol) of the Different Structures of Neutral and Ionized Glycine Computed at Different Levels with the D95++(d,p) Basis Set

	B3LYP	CCSD(T)//B3LYP	MP2	CCSD(T)//MP2	BHLYP	CCSD(T)//BHLYP
			Neutral			
I	−284.506833(0.0)	−283.764983(0.0)	−283.707945(0.0)	−283.765126(0.0)	−284.349950(0.0)	−283.763083(0.0)
II	−284.506448(0.24)	−283.763441(0.97)	−283.707093(0.53)	−283.763723(0.88)	−284.348336(1.01)	−283.761672(0.88)
III	−284.504511(1.46)	−283.762543(1.53)	−283.705745(1.38)	−283.762872(1.41)	−284.347366(1.62)	−283.760641(1.53)
IV	−284.504448(1.50)	−283.762759(1.39)	−283.705883(1.29)	−283.763015(1.32)	−284.347617(1.46)	−283.760811(1.43)
			Ionized			
II(+)	−284.161764(6.24)	−283.414499(12.37)	−283.358491(8.82)	−283.414796(12.49)	−283.995602(15.80)	−283.412674(12.61)
III(+)	−284.176541(−3.03)	−283.431073(1.97)	−283.366806(3.60)	−283.430413(2.69)	−284.015226(3.49)	−283.429864(1.82)
IV(+)	−284.171711(0.0)	−283.434211(0.0)	−283.372541(0.0)	−283.434693(0.0)	−284.020786(0.0)	−283.432763(0.0)

SCHEME 1

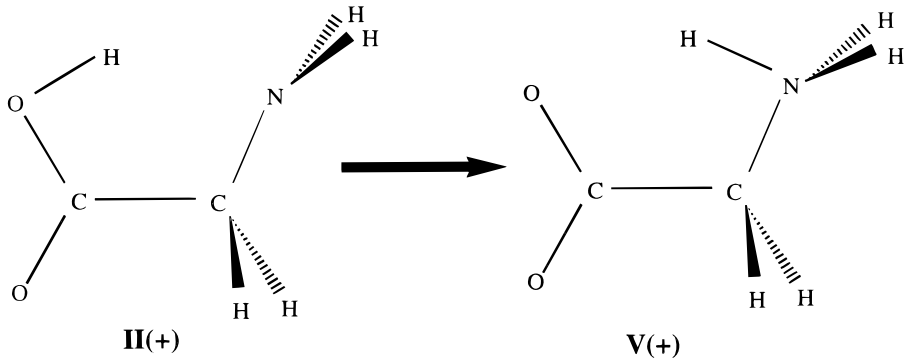

except the B3LYP one, structure **IV** is slightly more stable than structure **III**. It can be observed in Table 1 that also for these two structures the effect of the geometry on the CCSD(T) relative energies is small. That is, the computed CCSD(T) values differ by about 0.1 kcal/mol regardless of whether we use the B3LYP, MP2, or BHLYP geometries.

Figure 1 also shows the geomery of the radical cations derived from ionization of the four neutral conformers considered. The first thing to note is that only three stable structures are obtained upon ionization of structures **I**−**IV**. In particular, the radical cation corresponding to structure **I**, **I(+)**, has not been found to be a minimum on the potential energy surface. The optimization of ionized **I** leads to a stationary point with one imaginary frequency, which after symmetry relaxation evolved to structure **III(+)** at the B3LYP level or to structure **IV(+)** at the MP2 or BHLYP ones. As it can be observed in Table 1, all methods except the B3LYP, provide conformer **IV(+)** to be the most stable radical cation, in good agreement with the study of Yu et al.[8] At the B3LYP level, structure **III(+)** is found to be the lowest one. This discrepancy is not surprising considering that **III(+)** presents a three-electron bond between N and O. These structures have recently been found[36,39] to be overstabilized by present density functionals, due to an overestimation of the self-interaction part of the exchange energy because of the delocalized nature of the electron hole. These studies have shown that the admixture of exact exchange energy reduces the error and that the density functional approach that better compares to post-Hartree−Fock calculations is the BHLYP one. Table 1 shows also that, in the present case, the BHLYP method provides better results than B3LYP. Nevertheless, despite the geometry differences between B3LYP and MP2 for **III(+)**, the CCSD(T)//MP2 and CCSD(T)//B3LYP relative energies are similar. The adiabatic ionization potential of glycine computed using structures **I** and **IV(+)** is 9.0 eV at the CCSD(T) and BHLYP levels and 9.1 eV with the B3LYP and MP2 methods. These values are in very good agreement with the experimental one of 8.9 eV.[51]

The highest energy radical cation corresponds to structure **II(+)**, which in contrast to the neutral species, has C_s symmetry. The fact that conformer **II(+)** is less stable than **IV(+)** can be understood considering that the HOMO orbital from which the electron is removed has an important contribution from the lone pair of nitrogen. Thus, when the amino group is acting as a proton acceptor, **II(+)**, the hydrogen bond is weakend due to a decrease of the nitrogen basicity, whereas when it is acting as a proton donor, **IV(+)**, the ionization increases its acidity and the hydrogen bond is strengthened.

Although **II(+)** is not the most stable one, this structure is the one involved in the intramolecular proton transfer process in which we are interested. On the other hand, given the large geometry differences between the different radical cations, we expect the barriers to isomerization to be much larger than that of the proton-transfer process. Therefore, the initial population of **II(+)** is expected to be determined by that of the neutral parent and not by that of an equilibrium distribution of the ionized structures.

II. Intramolecular Proton-Transfer Process. In this work, we study the proton-transfer process in glycine radical cation shown in Scheme 1.

Figure 2 shows the optimized structures of the ionized species (minima and transition state) involved in the reaction. Structure **II(+)** presents C_s symmetry and the electronic state is $^2A'$. However, structure **V(+)** has C_s symmetry at the B3LYP and BHLYP levels of calculation and C_1 at the MP2 one. At the MP2 level, the C_1 structure is slightly distorted with respect to the C_s one, the energy difference being only 0.06 kcal/mol. The reaction energies and the energy barriers at different levels of theory are given in Table 2.

First of all, it is interesting to analyze the changes produced in **II** after ionization. It can be observed in Figure 1 that ionization of **II** increases significantly the C−C bond distance. This increase can be related to the nodal planes observed in the HOMO orbital of **II** (see Figure 3) from which the electron is removed. This orbital shows an important bonding character between both carbon atoms, and so it is not surprising that ionization increases the C−C distance. The changes observed

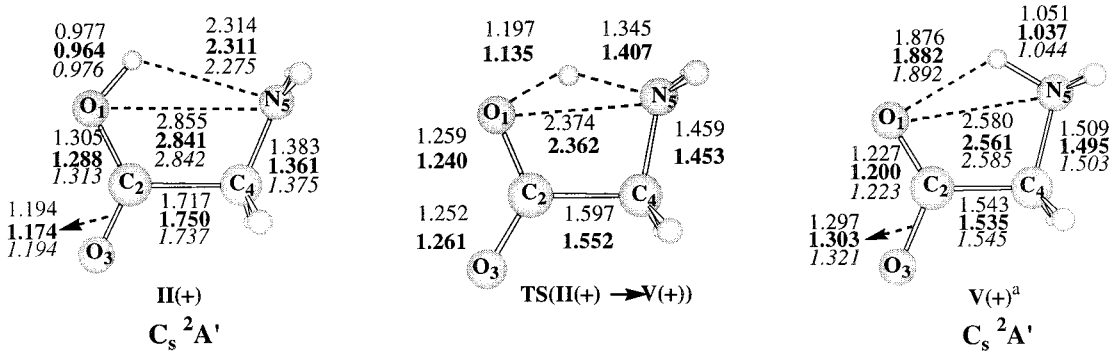

Figure 2. B3LYP, **BHLYP**, and *MP2* optimized geometries of ionized species involved in the proton-transfer process. Distances are in angstroms and angles are in degrees. [a] C_1 symmetry at the MP2 level.

TABLE 2: Relative Energies of Structures II(+) and V(+) Computed at Different Levels (in kcal/mol)

method	II(+)	TS(II(+) → V(+))	V(+)
B3LYP/D95++(d,p)	0.0	9.3	2.6
BHLYP/D95++(d,p)	0.0	2.9	−7.6
B3LYP/6-311+G(3df,2p)	0.0	12.3	4.9
MP2/D95++(d,p)	0.0	13.3[a]	1.6
CCSD(T)/D95++(d,p)//B3LYP/D95++(d,p)	0.0	5.8	−4.8
CCSD(T)/D95++(d,p)//BHLYP/D95++(d,p)	0.0	5.6	−5.3
CCSD(T)/6-311+G(3df,2p)// B3LYP/6-311+G(3df,2p)	0.0	9.0	−1.0

[a] Estimated value (see text).

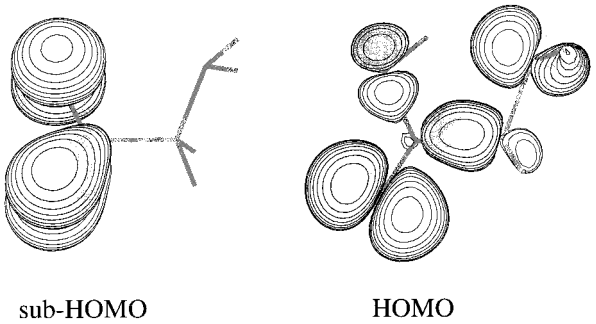

Figure 3. HOMO and sub-HOMO orbitals of glycine.

in the other geometrical parameters can also be understood by considering the nodal properties of the HOMO orbital.

The HOMO orbital is delocalized over the molecule, the most important contributions being in N_5 and O_3. In particular, this orbital has an important contribution of the lone pair of the proton acceptor nitrogen. Consequently, ionization decreases its basicity and the hydrogen bond becomes less favorable which produces an important increase of the hydrogen bond distance. Natural population analysis indicates that the spin density is 0.43 for N_5 and 0.38 for O_3. After the hydrogen is transferred to the nitrogen atom, structure **V(+)** in Figure 2, the hydrogen bond is strengthened. Now, the radical character moves completely to O_3 (the spin density over O_3 is 0.91), since this allows O_1 to participate in the hydrogen bond with two electrons. Therefore, the hydrogen bond becomes more favorable and the hydrogen bond distance decreases.

It can also be observed in Table 2 that the barrier of the hydrogen transfer process is appreciable at all levels of theory, in such a way that the reaction shows always a double well profile. However, it is worth noting that B3LYP and BHLYP show a different behavior. While at the B3LYP level, the reaction is endothermic, at the BHLYP level it is exothermic. Despite this, the CCSD(T) results using the B3LYP geometry (−4.8 kcal/mol) or the BHLYP one (−5.3 kcal/mol) are very similar and show that the reaction is exothermic. The energy barrier for the considered reaction also shows different behavior between both functionals. That is, whereas the B3LYP method overestimates the energy barrier, compared to CCSD(T), the value obtained at the BHLYP level is underestimated. The observed trend is in agreement with the Hammond postulate. However, the values obtained at the CCSD(T) level are also very similar with both geometries. Thus, both B3LYP and BHLYP density functional methods provide reasonable geometries for the different stationary points. To test the effect of further expanding the basis set, we have also performed B3LYP and single-point CCSD(T) calculations with the 6-311+G(3df,-2p) basis. The B3LYP results show that the reaction is more endothermic and accordingly the energy barrier increases. A similar variation is observed at the CCSD(T) level. Finally, MP2 results provide a reaction energy that is similar to B3LYP but a higher barrier, as it is often observed. It should be noted that the MP2 energy barrier has been estimated from several calculations around the transition state structure since direct localization has been shown to converge very slowly. Because of that, we have not performed single-point calculations at the CCSD(T) level using MP2 geometries to compute the energy barrier. The reaction energy at the CCSD(T)//MP2 level (−5.0 kcal/mol) is, however, very similar to that obtained at the CCSD-(T)//B3LYP one (−4.8 kcal/mol).

Figure 4 shows the energy profiles of the reaction obtained with different methods. For the sake of comparison, the HF results have been added. It can be observed that, at the BHLYP level, in addition to the two minima shown in Figure 2, there is an intermediate on the potential energy surface. In this intermediate, the spin density has already been localized over O_3 (0.82), similar to the situation in the **V(+)** product where the radical character lies on the carboxylic group but the hydrogen has not yet been transferred. As a consequence, the hydrogen bond becomes more favorable and the N_5−H distance decreases significantly (1.884 Å). It should be noticed, however, that the CCSD(T)//BHLYP energy of the transition state that connects the conformer **II(+)** and the intermediate is lower than the CCSD(T)//BHLYP energy of the intermediate, thus indicating that the presence of this new minimum is an artifact of the BHLYP method.

It is also interesting to note that the HF method also shows the presence of this intermediate, but in this case it is 9.9 kcal/mol more stable than the **II(+)** conformer. From these results, it can be deduced that the existence of this intermediate at the BHLYP level is due to the excessive amount of HF exchange mixing (∼50%)in the functional. On the other hand the B3LYP method, where the mixing of HF exchange is smaller (∼20%), solves this problem, and only three stationary points appear on

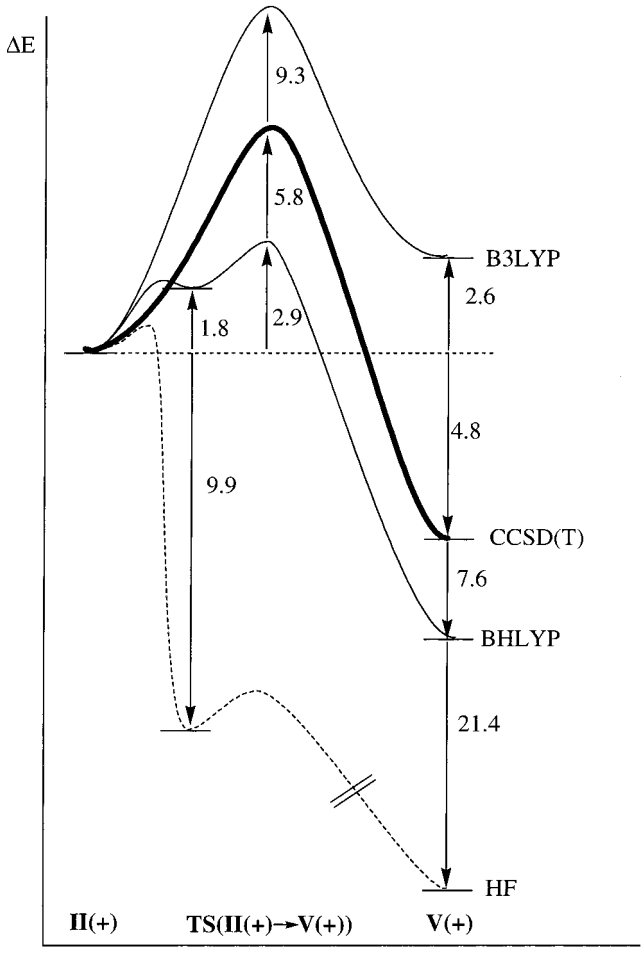

Figure 4. Energy profile of the proton-transfer process in the $^2A'$ state computed at different levels of calculation. Energies are in kcal/mol.

the potential energy surface. However, the B3LYP method does not reproduce correctly the energetic differences compared to the CCSD(T) method. In other words, depending on the method, one can obtain artificial structures, and so it is always desirable to confirm the DFT results for the energy, when possible, by performing calculations with highly correlated ab initio methods. From Figure 4, one might expect that a functional with a mixing between BHLYP and B3LYP would provide results much closer to the CCSD(T) method.

Up to present, we have considered the proton-transfer process in the lowest ionized state of glycine. However, a very different behavior is expected if ionization is produced in the sub-HOMO orbital of **II**. Given that for **II** the C_1 structure is only slightly distorted from the C_s one, we have imposed C_s smmetry in order to study this second ionic state ($^2A''$) at the B3LYP level. We expect that this restriction will not perturb essentially the energy profile and would be a good aproximation to study the intramolecular proton transfer in this second ionic state, which lies about 30 kcal/mol above the lowest $^2A'$ state. Geometry optimization of the $^2A''$ state produces the spontaneous transfer of the hydrogen, and so only the proton transferred structure is found.

It can be observed in Figure 3 that the sub-HOMO orbital is completely localized at the carboxylic group. Therefore, after ionization from this orbital, the acidity of the carboxylic group increases. Thus, it is not surprising that in this $^2A''$ state, ionization produces the spontaneous transfer of the hydrogen, leading to a structure similar to **V(+)**. This structure lies about 11.2 kcal/mol above **V(+)**. However, in contratst to **V(+)**, the

TABLE 3: Natural Population Analysis of Ionized Species Involved in the Proton-Transfer Process

		reactant			product		
		COOH	CH_2	NH_2	COO	CH_2	NH_3
$^2A''$	charge	0.79[a]	0.27[a]	−0.06[a]	0.1	0.24	0.66
	spin dens.	0.98[a]	0.02[a]	0.00[a]	1.0	0.0	0.0
$^2A'$	charge	0.46	0.3	0.24	0.1	0.25	0.65
	spin dens.	0.49	0.1	0.41	0.99	−0.01	0.02

[a] Values determined optimizing the nontransferred conformer of the $^2A''$ state of ionized glycine with the O−H distance frozen at 1.0 Å.

obtained hydrogen transferred structure in the $^2A''$ state presents a very small imaginary frequency (67 cm^{-1}) that corresponds to an out-of-plane movement (a″) of the hydrogen atoms. We have not been able to obtain the corresponding minimum since, relaxing the symmetry constraints, the B3LYP method collapses to the ground electronic state which converges to the planar **V(+)** $^2A'$ structure. Although we expect that the corresponding minimum would only be slightly distorted compared to that obtained with C_s symmetry due to the small value of the imaginary frequency, the existence of this structure remains open.

Let us now discuss the nature of the hydrogen transfer in glycine radical cation. Table 3 shows the natural population analysis of the reactant and product of ionized glycine in both $^2A'$ and $^2A''$ states. It can be observed that the initial situation is very different in both states. In the $^2A''$ state the charge and the spin density are localized in the carboxylic group, the spin density being mainly over O_3 (0.82). After the hydrogen has been transferred, the spin density is still localized in the carboxilic group but the charge has moved to the amino group. Thus, the process can be viewed as the transfer of a proton from the carboxylic group to the amino group and the final picture of the system is the typical situation of a distonic radical. In the initial **II(+)** structure of the $^2A'$ state, the spin density is mainly centered in the carboxylic and the amino groups while the charge is delocalized over the molecule. However, in the final product **V(+)** the situation is almost the same as that in the $^2A''$ state (see Table 3). In this case, the charge over the amino group increases from 0.24 to 0.65 while in the $^2A''$ state varies from −0.06 to 0.66. Therefore, the process in the $^2A'$ state could be viewed as a proton-transfer accompanied by an important electronic reorganization. The result of this reorganization resembles an electronic transfer from the oxygen O_3 to the nitrogen which produces significant changes in the spin densities and atomic charges. For instance, the spin density in O_3 varies from 0.38, in the reactant, to 0.91 in the product and the charge changes from −0.34 to −0.14. As a consequence, the final structure has the same distonic radical character than the $^2A''$ state.

In summary, in the $^2A''$ state, the electronic distribution of the system does not change significantly during the process except that a proton is transferred. Because of that, and the high exothermicity of the reaction, the process takes place spontaneously. In contrast, in the $^2A'$ state, there is an important electronic reorganization during the reaction which implies the appearance of an energy barrier. However, the final situation is the same in both cases: a distonic radical.

Conclusions

Ionization of the four lowest conformers of glycine, **I**−**IV**, leads to three stable ionic structures, **II(+)**−**IV(+)**. Ionization of **I** leads to a first-order saddle point that evolves to structure **IV(+)**. The energy ordering of the ionized species differs from

that observed for the neutral ones. In particular, **II(+)** becomes significantly less stable than **IV(+)**. This is due to the fact that the intramolecular hydrogen bond is weakened when the amino group acts as a proton acceptor, **II(+)**, whereas it is strengthened when it is acting as a proton donor, **IV(+)**.

Ionization of **II(+)** favors the proton-transfer process. That is, whereas in the gas phase the zwitterionic form of glycine [$NH_3^+-CH_2-COO^-$] does not exist, for glycine radical cation the proton-transferred structure [$NH_3^+-CH_2-COO^\bullet$], **V(+)**, is similar in energy to the nontransferred one [$NH_2-CH_2-COOH]^+$, **II(+)**. For the $^2A'$ ground state, we have localized the reactant, product, and transition state, the energy barrier being about 9 kcal/mol at our best level of calculation. The sign of the energy difference between the reactant and product is different depending on the level of theory. At the BHLYP level, an additional intermediate corresponding to a nontransferred structure but with a strong intramolecular hydrogen bond is found. This minimum is an artifact of the method, and some caution needs to be taken when dealing with these kinds of systems, since depending on the starting point, the system can collapse to one minimum with a strong hydrogen bond or to another one with a weak hydrogen bond.

The proton transfer process in glycine radical cation is different in the ground and in the first excited state. In the first case, there is a barrier for the proton transfer, while in the excited state, the proton transfer appears to be spontaneous. Nevertheless, the final situation is similar in both cases: the proton transferred structure has the nature of a distonic radical, with the spin density mainly localized in the carboxylic group and the charge localized in the amino group.

Acknowledgment. Financial support from DGICYT, through the PB95-0640 project, and the use of the computational facilities of the Catalonia Supercomputer Center are gratefully acknowledged.

References and Notes

(1) Jensen, J. H.; Gordon, M. S. *J. Am. Chem. Soc.* **1995**, *117*, 8159.
(2) Tortonda, F. R.; Pascual-Ahuir, J. L.; Silla, E.; Tuñón, I.; Ramírez, F. J. *J. Chem. Phys.* **1998**, *109*, 592.
(3) Okuyama-Yoshida, N.; Nagaoka, M.; Yamabe, T. *J. Phys. Chem. A* **1998**, *102*, 285.
(4) Nagaoka, M.; Okuyama-Yoshida, N.; Yamabe, T. *J. Phys. Chem. A* **1998**, *102*, 8205.
(5) Tuñon, I.; Silla, E.; Millot, C.; Martins-Costa, T. C.; Ruiz-López, M. F. *J. Phys. Chem. A* **1998**, *102*, 8673.
(6) Schäfer, L.; Sellers, H. L.; Lovas, F. J.; Suenram, R. D. *J. Am. Chem. Soc.* **1980**, *102*, 6566.
(7) Jensen, J. H.; Gordon, M. S. *J. Am. Chem. Soc.* **1991**, *113*, 7917.
(8) Yu, D.; Armstrong, D. A.; Rauk, A. *Can. J. Chem.* **1992**, *70*, 1762.
(9) Vijay, A.; Sathyanarayana, D. N. *J. Phys. Chem.* **1992**, *96*, 10735.
(10) Frey, R. F.; Coffin, J.; Newton, S. Q.; Ramek, M.; Cheng, V. K. W.; Momany, F. A.; Schäfer, L. *J. Am. Chem. Soc.* **1992**, *114*, 5369.
(11) Császár A. G. *J. Am. Chem. Soc.* **1992**, *114*, 9568.
(12) Hu, C.-H.; Shen, M.; Schaefer, H. F., III *J. Am. Chem. Soc.* **1993**, *115*, 2923.
(13) Lelj, F.; Adamo, C.; Barone, V. *Chem. Phys. Lett.* **1994**, *230*, 189.
(14) Godfrey, P. D.; Brown, R. D. *J. Am. Chem. Soc.* **1995**, *117*, 2019.
(15) Gordon, M. S.; Jensen, J. H. *Acc. Chem. Res.* **1996**, *29*, 536.
(16) Sirois, S.; Proynov, E. I.; Nguyen, D. T.; Salahub, D. R. *J. Chem. Phys.* **1997**, *107*, 6770.
(17) Zhang, K.; Chung-Phillips, A. *J. Phys. Chem. A* **1998**, *102*, 3625.
(18) Stepanian, S. G.; Reva, I. D.; Radchenko, E. D.; Rosado, M. T. S.; Duarte, M. L. T. S.; Fausto, R.; Adamowicz, L. *J. Phys. Chem. A* **1998**, *102*, 1041.
(19) Ding, Y.; Krogh-Jespersen, K. *Chem. Phys. Lett.* **1992**, *199*, 261.
(20) Chakraborty, D.; Manogaran, S. *Chem. Phys. Lett.* **1998**, *294*, 56.
(21) Rauk, A.; Yu, D.; Armstrong, D. A. *J. Am. Chem. Soc.* **1998**, *120*, 8848.
(22) Stadman, E. R. *Annu. Rev. Biochem.* **1993**, *62*, 797.
(23) Sies, H. *Oxidative Stress—Oxidants and Anti-Oxidants*; Academic Press: London, 1991.
(24) Simic, M. G.; Taylor, K. A.; Ward, J. F.; Von Sonntag, C. *Oxygen radicals in Biology and Medicine*; Plenum Press: New York, 1988.
(25) Davies, K. J. A. *Oxidative Damage and Repair: Chemical, Biological and Medical Aspects*; Pergamon Press: New York, 1991.
(26) von Sonntag, C. *The Chemical Basis of Radiation Biology*; Taylor and Francis: London, 1987.
(27) Leroy, G.; Sana, M.; Wilant, C. *J. Mol. Struct.* **1991**, *228*, 37.
(28) Barone, V.; Adamo, C.; Grand, A.; Subra, R. *Chem. Phys. Lett.* **1995**, *242*, 351.
(29) Yu, D.; Rauk, A.; Armstrong, D. A. *J. Am. Chem. Soc.* **1995**, *117*, 1789.
(30) Barone, V.; Adamo, C.; Grand, A.; Brunel, Y.; Fontecave, M.; Subra, R. *J. Am. Chem. Soc.* **1995**, *117*, 1083.
(31) Barone, V.; Adamo, C.; Grand, A.; Jolibois, F.; Brunel, Y.; Subra, R. *J. Am. Chem. Soc.* **1995**, *117*, 12618.
(32) Rega, N.; Cossi, M.; Barone, V. *J. Am. Chem. Soc.* **1997**, *119*, 12962.
(33) Rega, N.; Cossi, M.; Barone, V. *J. Am. Chem. Soc.* **1998**, *120*, 57323.
(34) (a) Sodupe, M.; Oliva, A.; Bertran, J. *J. Phys. Chem. A* **1997**, *101*, 9142. (b) Bertran, J.; Oliva, A.; Rodríguez-Santiago, L.; Sodupe, M. *J. Am. Chem. Soc.* **1998**, *120*, 8159.
(35) (a) Baker, J.; Scheiner, A.; Andzelm, J. *Chem. Phys. Lett.* **1993**, *216*, 380. (b) Barone, V.; Adamo, C. *Chem. Phys. Lett.* **1994**, *224*, 432.
(36) Sodupe, M.; Bertran, J.; Rodríguez-Santiago, L.; Baerends, E. J. *J. Phys. Chem. A* **1999**, *103*, 166.
(37) Mohr, M.; Zipse, H.; Marx, D.; Parrinello, M. *J. Phys. Chem. A* **1997**, *101*, 8942.
(38) Bickelhaupt, F. M.; Diefenbach, A.; Visser, S. P.; Koning, L. J.; Nibbering, N. M. M. *J. Phys. Chem. A* **1998**, *102*, 9549.
(39) Braïda, B.; Hiberty, P. C.; Savin, A. *J. Phys. Chem. A* **1998**, *102*, 7872.
(40) Lee, C.; Yang, W.; Parr, R. G. *Phys. Rev. B* **1988**, *37*, 785.
(41) Becke, A. D. *J. Chem. Phys.* **1993**, *98*, 5648.
(42) Becke, A. D. *J. Chem. Phys.* **1993**, *98*, 1372.
(43) Raghavachari, K.; Trucks, G. W.; Pople, J. A.; Head-Gordon, M. *Chem. Phys. Lett.* **1989**, *57*, 479.
(44) Dunning, T. H. *J. Chem. Phys.* **1970**, *53*, 2823.
(45) Frisch, M. J.; Trucks, G. W.; Schlegel, H. B.; Gill, P. M. W.; Johnson, B. G.; Robb, M. A.; Cheeseman, J. R.; Keith, T.; Petersson, G. A.; Montgomery, J. A.; Raghavachari, K.; Al-Laham, M. A.; Zakrzewski, V. G.; Ortiz, J. V.; Foresman, J. B.; Cioslowski, J.; Stefanov, B. B.; Nanayakkara, A.; Challacombe, M.; Peng, C. Y.; Ayala, P. Y.; Chen, W.; Wong, M. W.; Andres, J. L.; Replogle, E. S.; Gomperts, R.; Martin, R. L.; Fox, D. J.; Binkley, J. S.; Defrees, D. J.; Baker, J.; Stewart, J. P.; Head-Gordon, M.; Gonzalez, C.; Pople, J. A. *Gaussian 94*, revision D.1; Gaussian Inc.: Pittsburgh, PA, 1995.
(46) Reed, A. E.; Curtiss, L. A.; Weinhold, F. *Chem. Rev.* **1988**, *88*, 899.
(47) MOLPRO is a package of ab initio programs written by H. J. Werner and P. J. Knowles, with contributions from, J. Almlöf, R. D. Amos, A. Berning, D. L. Cooper, M. J. O. Deegan, A. J. Dobbyn, F. Eckert, S. T. Elbert, C. Hampel, R. Lindh, W. Lloyd, W. Meyer, A. Nicklass, K. Peterson, R. Pitzer, A. J. Stone, P. R. Taylor, M. E. Mura, P. Pulay, M. Schütz, H. Stoll, and T. Thorsteinsson. The RCCSD program is described in the following: Knowles, P. J.; Hampel, C.; Werner, H.-J. *J. Chem. Phys.* **1993**, *99*, 5219.
(48) Barone, V.; Adamo, C.; Lelj, F *J. Chem. Phys.* **1995**, *102*, 364.
(49) Császár, A. G. *J. Mol. Struct.* **1995**, *346*, 1789.
(50) Suenram, R. D.; Lovas, F. *J. Am. Chem. Soc.* **1980**, *102*, 7180.
(51) Cannington, P. H.; Ham, N. S. *J. Electron. Spectrosc. Relat. Phenom.* **1983**, *32*, 139.